Computational optimisation of optical projection tomography for 3D image analysis

Tang, X.

Citation

Tang, X. (2020, June 10). *Computational optimisation of optical projection tomography for 3D image analysis*. Retrieved from https://hdl.handle.net/1887/106088

Cover Page

Universiteit Leiden

Author: Tang, X.
Title: Computational optimisation of optical projection tomography for 3D image analysis
Issue Date: 2020-06-10

Chapter 6

Exploration of 3D Structure Annotation and Visualization of Zebrafish Reconstructions from Optical Projection Tomography Imaging

Chapter summary

In this chapter we investigate the last parts of 3D optical projection tomography imaging pipeline: annotation and visualization. Our results focus on zebrafish samples without specific staining from the bright-field channel of the OPT. With respect to annotation, we first present the manual method from different software packages including our own annotation software. This provides a clue about how much 3D information within zebrafish can be obtained from the optical projection tomography 3D imaging system. Beside manual annotation, an automated 3D annotation method is explored to give an insight in the extent to which deep learning can automate 3D annotation process. With the results the limitations are analysed and new perspectives are presented.

6.1 Introduction

The zebrafish is an important vertebrate model organism that is widely used in biomedical research, e.g. developmental biology, disease biology, toxicology and behaviour. In this research, the identification and quantification of marker signals from genes and proteins have been providing basic evidence for gene analysis [133].

Detailed analysis of genes includes the identification of certain proteins in organs rather than looking at a whole-mount study of zebrafish [134]. Moreover, these organs can be physically dissected for an individual proteomic analysis [134]–[137]. Such techniques aim to answer the questions, e.g. is a gene X is expressed in an organ and how much of the corresponding proteins can be identified in this organ. From imaging, and multi-channel OPT in particular, expression patterns can be visualized *in situ* so that location and distribution of genes and proteins can be established.

Spatial analysis of patterns of gene expression from whole-mount zebrafish has been applied in the last decades [11], [138]–[141]. This has often been done using *in situ* hybridization (ISH). In this manner the localization of gene-expression has been accomplished. However, research on detailed analysis within organs is limited by the techniques available for the imaging of organs and subsequent annotation. To overcome these limitations, we explore annotation with experiments to detect zebrafish organs or volume regions from optical projection tomography (OPT).

In the application of imaging with OPT, we assume that patterns of gene expression can be visualized in the fluorescence channel through fluorescent *in situ* hybridization (FISH) or using a fluorescent reporter gene (e.g. GFP) . In general, the bright-field channel provides structural information for zebrafish and this includes some of the organs. Our research questions therefore are: (1) to what extent the organs or volume regions can be annotated from OPT 3D images of whole-mount zebrafish; (2) to what extent this annotation process can be automated.

In order to answer these questions, we have manually annotated 5 *dpf* and 25 *dpf* zebrafish from 3D images obtained from the OPT imaging system. In addition, automated annotation is explored on the 5 *dpf* zebrafish for the annotation of 4 labels. The results of the annotation are presented with different visualization software packages.

In order to set the terminology right for the remainder of this chapter, three definitions are introduced. First, we define (1) *The anatomical domain* as a demarcation of an anatomical structure and this structure is being generally accepted as a named structure in anatomy of a species. We consider (2) named structures to follow unambiguous labels that are organised in *controlled vocabularies* or *curated ontologies*. An annotation label for an anatomical domain is extracted from either of these curated namespaces. In addition to the anatomical domains we distinguish (3) *the volume region* as volumetric part of an organism presenting a dedicated region that is not coinciding with a recognized anatomical domain but it can be addressed for its named location.

With these definitions in hand we can make annotation in zebrafish with the intention to detect volume regions and anatomical domains that can be found in the bright-field 3D image without any specific contrast techniques being employed.

This chapter is structured as follows. In section 6.2 we will introduce the sample preparation, the OPT imaging system, the annotation methods and the visualization software. In section 6.3 we explain the annotation and experiment with visualization using different software packages. The results include both manual and automated annotation methods. Conclusions and discussion are summarized in section 6.4.

6.2 Methods and materials

In order to visualize and quantify a region of interest within a zebrafish, samples need to be first prepared and imaged. With the tomograms acquired from the OPT imaging system, 3D reconstruction is applied to obtain a 3D image. This 3D image is used for segmentation to find the structures for annotation, e.g. zebrafish *Eye* that can subsequently be visualized as a label. The workflow is shown in Figure 6.1.
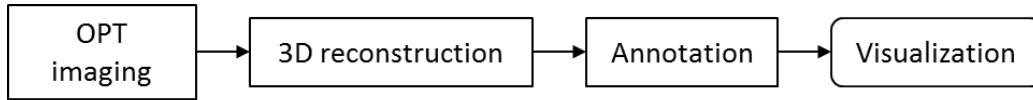

Figure 6.1. The workflow summary of OPT 3D imaging system.

6.2.1 Zebrafish and OPT 3D imaging system

During zebrafish development from larva to juvenile, structures and organs become more distinct and can be visualised using the OPT imaging system. In order to visualize and compare them, we use a 5 *dpf* and a 25 *dpf* zebrafish for our experiments. Each sample is prepared with the BABB or the CUBIC protocol (cf. § 4.4.2). The samples are prepared and imaged only with the clearing solution for the sole purpose of making the specimen transparent. No additional staining is used, meaning that the 3D structures of the zebrafish that we can obtain from our OPT imaging system represent the minimum information. With a counterstaining or a specific staining, the visualization of more structures can be accomplished. The OPT imaging system and reconstruction configurations as described in § 5.2.2 are used.

6.2.2 Annotation method

With the 3D image obtained from the reconstruction, manual annotation is first considered to provide a clue about how much 3D information within zebrafish can be identified without staining, using the OPT imaging on both zebrafishes. A manual annotation of the 3D image is accomplished with annotation software, e.g. Amira [63], TDR-3Dbase [12]–[14], Vaa3D [144], etc. In our work, Amira and TDR-3Dbase software are used for manual annotation. Aside from the manual annotation, we also explore the possibility of automated annotation for the visualization. The approach we used for the

automated annotation is semantic segmentation using the 3D U-net, which is set up according to chapter 5 (cf. § 5.3). Differently, multi-label segmentation rather than binary segmentation (cf. § 5.3) is required.

6.2.3 Visualization software

With respect to the descriptive parameters for phenotype characterisation of a volume region within zebrafish, visualization supports the qualitative information of the shape, size and context. Quantitative information is obtained from image analysis software. For visualization we use Amira [63], TDR-3Dbass [132], [142], [143] and MeshLab [145] software to visualize the individual regions in the 3D image, using several annotation methods.

6.3 Experiments

The first experiment is a manual annotation of zebrafish of different developmental stages and subsequent visualization of the annotated volume regions from the 3D OPT images. This aims to answer the question on the extent to which organs and/or volume regions can be annotated from a whole-mount zebrafish 3D image. The second part of the experiments focuses on the exploration of automated 3D annotation in 5 *dpf* zebrafish. As the 25 *dpf* zebrafish has more visible structures but fewer samples, the automated annotation of all parts is more challenging. Therefore, we start a simple with the 5dpf zebrafish that has much less distinct anatomical domains.

6.3.1 Manual annotation and visualization

   1) Amira

      In order to visualize a *5dpf* zebrafish in 3D or further do quantitative analysis on it, as a point of departure, the bright-field tomogram from the OPT imaging system is used. This tomogram consists of 400 images in our OPT setup. In Figure 6.2 (a) the tomogram is depicted that composes the input for the reconstruction algorithm. By using an effective reconstruction algorithm (cf. § 4.2), the tomogram is transposed to a raw 3D volumetric image of the zebrafish with a reduced amount of artefacts/noise. The raw 3D image is manually annotated and visualized using Amira [63] software (Figure 6.2 (b)). For volume region quantification in zebrafish annotation is required. Figure 6.2 (c) expresses an intuitive concept of 3D volume region segmentation or detection on a 5 *dpf* zebrafish. Obvious annotation labels are the zebrafish *Eye*, *Head*, *Muscle* and *Belly*; the latter three are location domains whereas Eye is an anatomical domain. The volume regions in this example are obtained based on manual segmentation of raw 3D image and subsequently visualized using Amira. Because of young age, transparency, and preparation method, most internal organs are not very well visible for zebrafish at this stage.
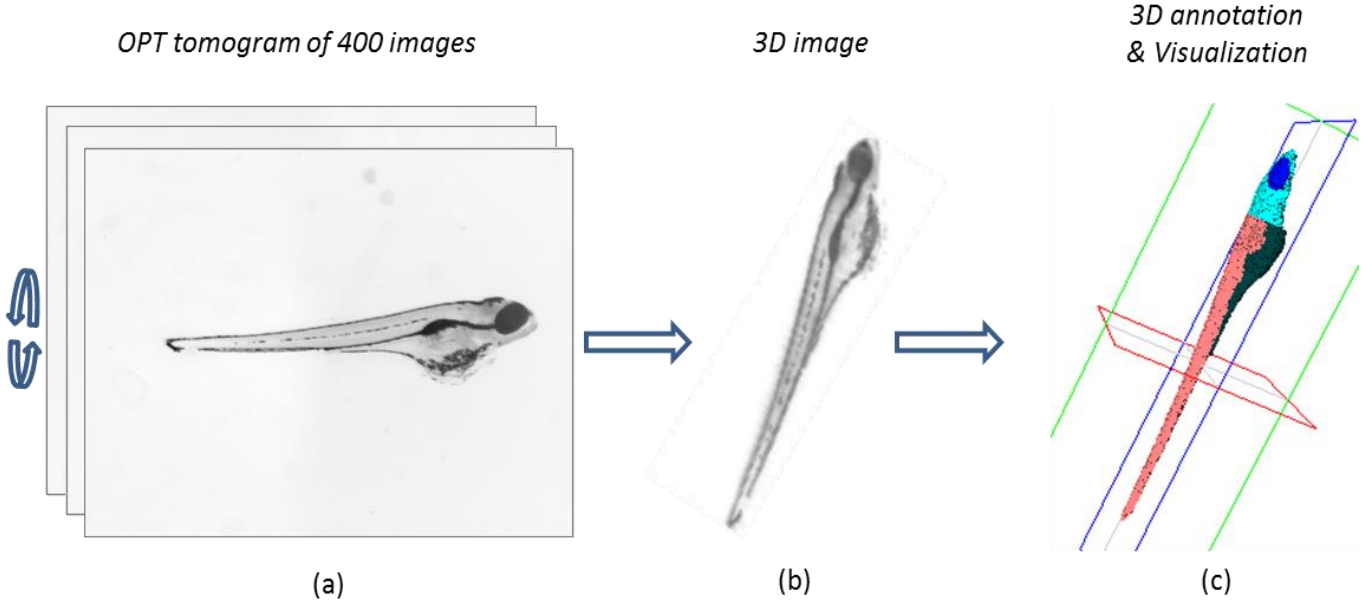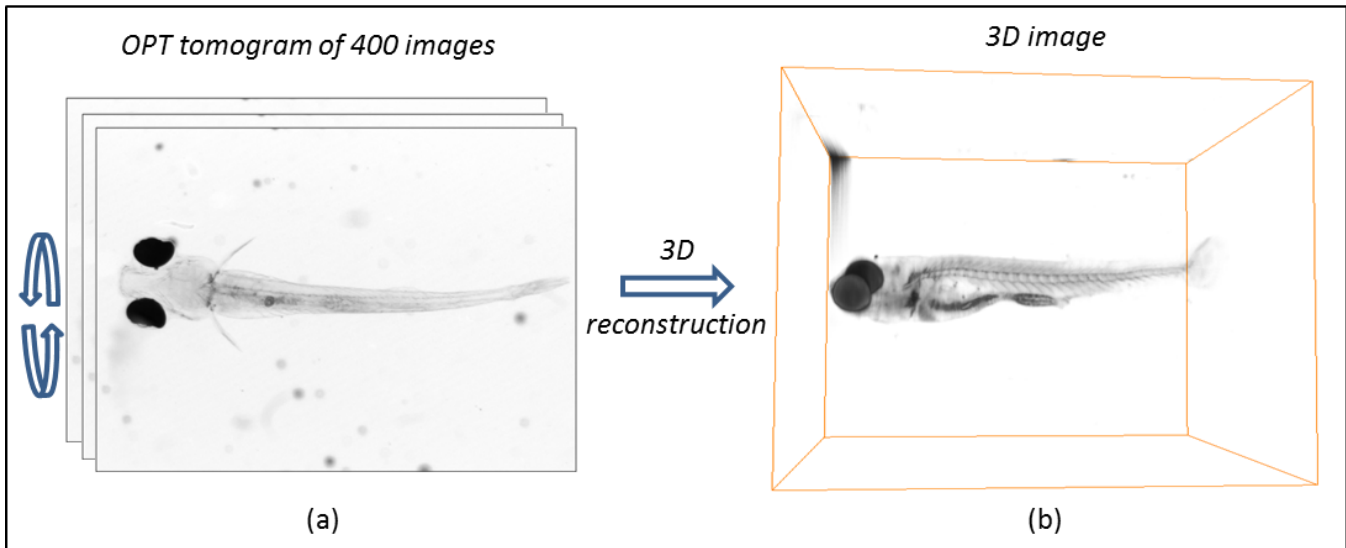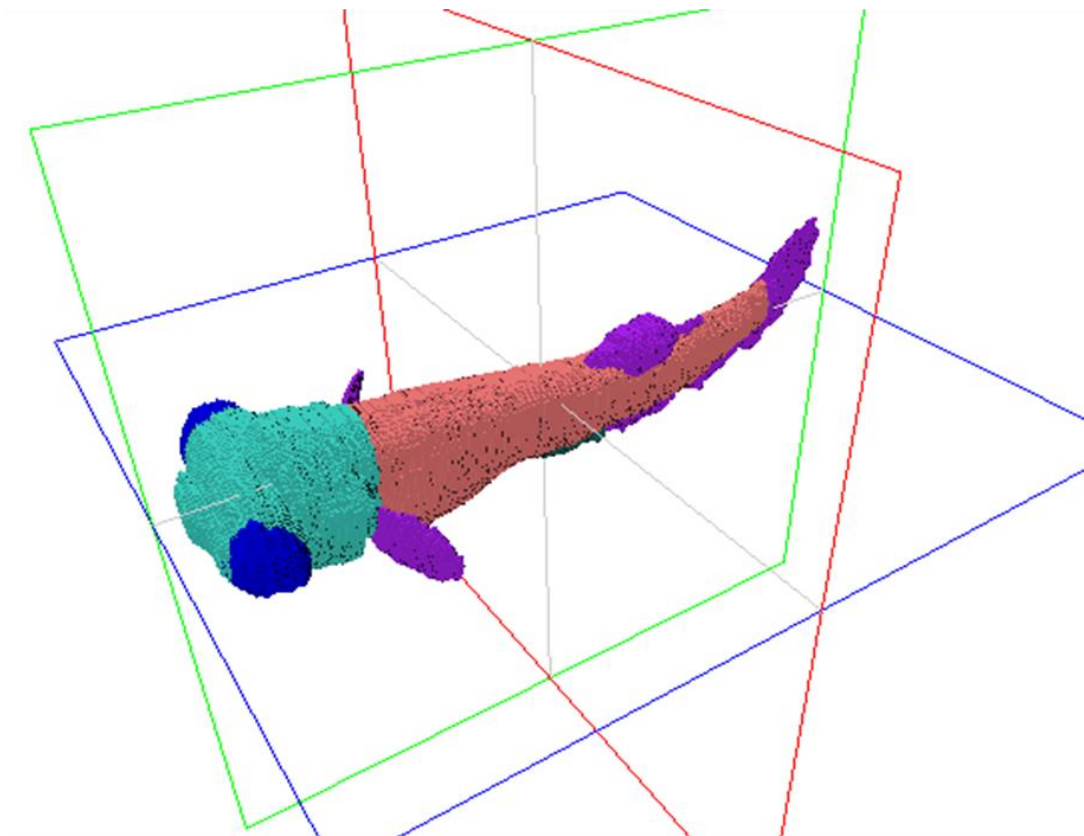
Figure 6.2. Workflow for 3D OPT imaging, reconstruction and segmentation on a 5 *dpf* zebrafish. (a) OPT tomogram of 400 images over 360° in OPT used for reconstruction. (b) Reconstructed 3D image from the 3D reconstruction algorithm. (c) Manually annotated 4 volumetric parts: *Eye* (blue), *Head* (light blue), *Muscle* (pink) and *Belly* (dark green).

Different from the 5 *dpf* zebrafish embryo in Figure 6.2, in Figure 6.3 the result of the imaging of a 25 *dpf* zebrafish with more internal structures is depicted. After reconstruction and semantic segmentation, the visualization is realized. This sample, i.e. tomogram, contains quite some noise, resulting in more background noise in the reconstruction as we can see from Figure 6.3 (b). The visualization results of the reconstruction are achieved by using a threshold in Amira as for 5 *dpf* zebrafish in Figure 6.2. The volume regions and anatomical domains we can distinguish from this sample are 9 different parts: *Eye* (blue), *Head* (light blue), *Muscle* (pink) and *Fin* (purple) in Figure 6.3 (c); *Blood vessel* (red) and *Belly* (dark green) in Figure 6.3 (d); *Notochord & Spinal cord* (yellow), *Swim bladder* (green) and *Intestine* (brown) in Figure 6.3 (e). As we can see, the *Swim bladder* has shrunk as a result of deflation. The volume regions and anatomical domains can provide significant information such as location or reference for fluorescent markers. It helps to understand volumetric structures of zebrafish in the OPT imaging system. Each individual part of the 25 *dpf* zebrafish is shown in Figure 6.4, using a surface rendering technique for visualization.

OPT tomogram of 400 images

3D reconstruction

3D image

(a)

(b)

3D annotation v1

(c)

3D annotation v2
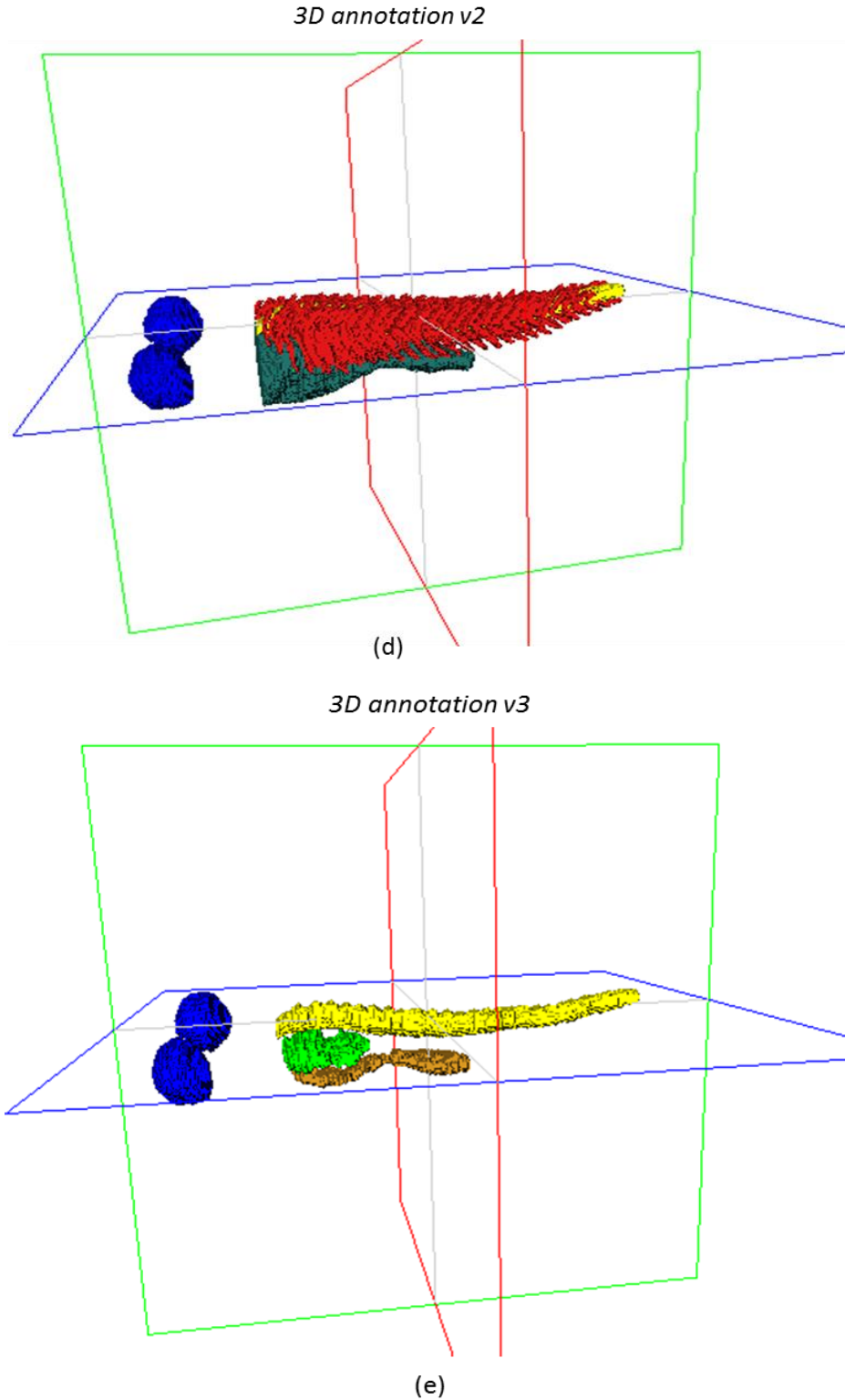

(d)

3D annotation v3

(e)

Figure 6.3. 3D OPT imaging, reconstruction and annotation on a 25 *dpf* zebrafish. (a) and (b) showing the projections and reconstruction respectively. (c), (d) and (e) visualizing 9 parts of zebrafish: *Eye*, *Head*, *Fin*, *Muscle*, *Blood vessels*, *Belly*, *Notochord & Spinal cord* (*N&SC*), *Swim bladder* (*SB*) and *Intestine*. V1, v2 and v3 represent three visualizations with increasing depth from outside to inside, with v1 showing the *Eye*, *Head*, *Fin* and *Muscle*, v2 showing the *Blood vessels* and *Belly*, and v3 showing the *N&SC*, *SB* and *Intestine*.
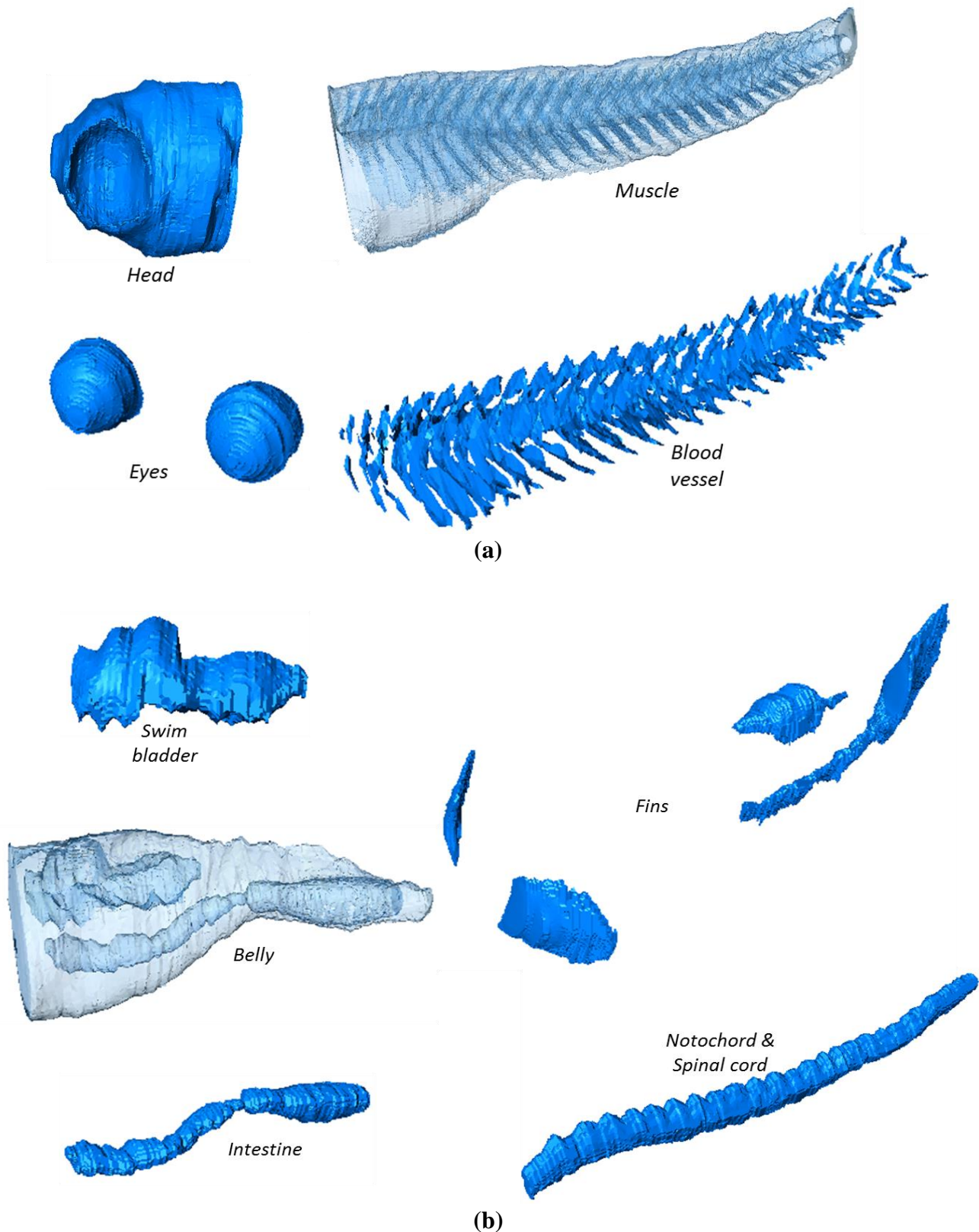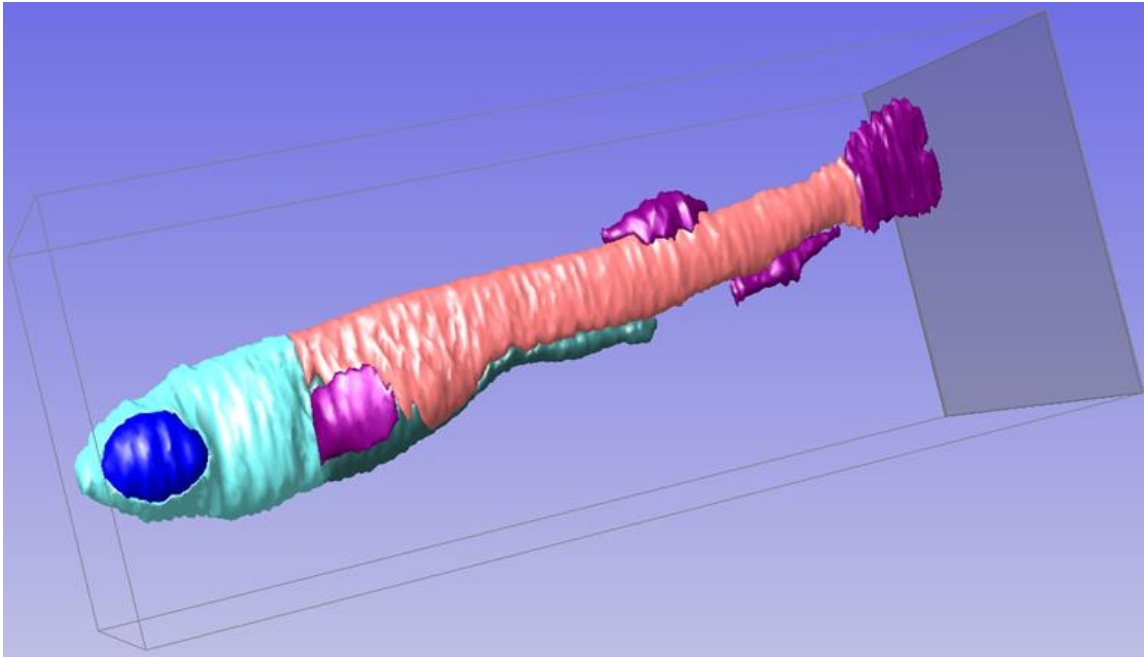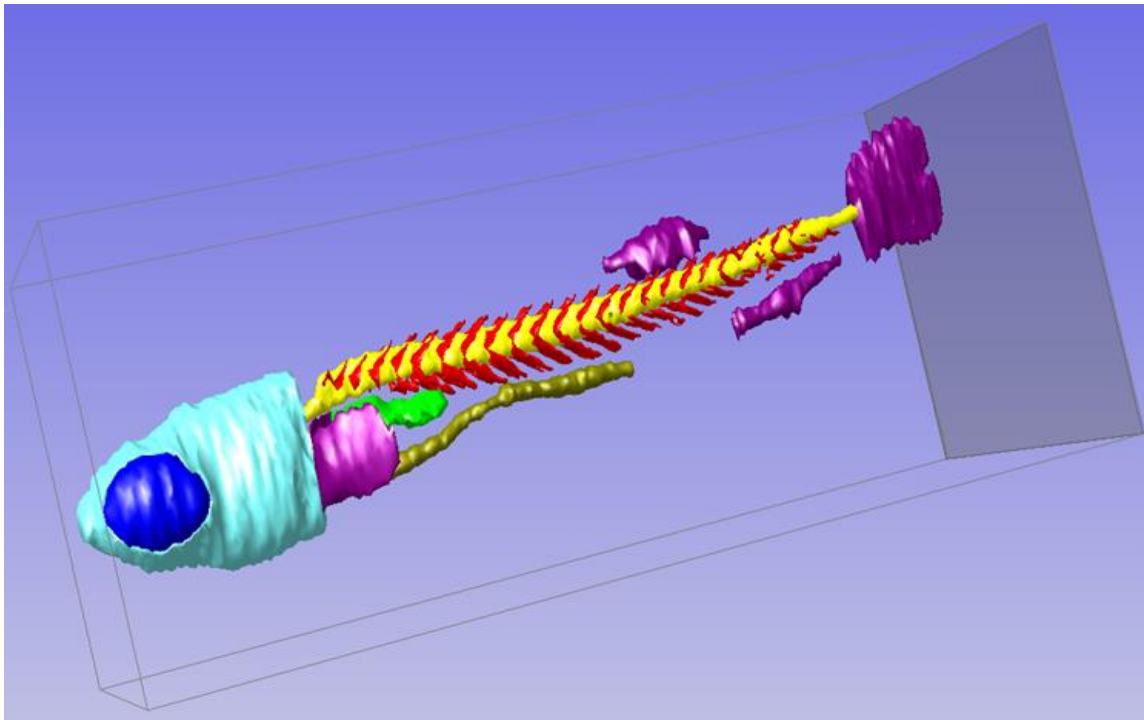
(a)

(b)

Figure 6.4. The individual part of the 25 *dpf* zebrafish. (a) The parts of *Head*, *Eye*, *Muscle* and *Blood vessel*, with *Muscle* being visualized transparently. (b) The parts of *Swim bladder*, *Belly*, *Intestine*, *Fin* and *Notochord & Spinal cord*, with *Belly* being visualized transparently.

(a)

(b)

Figure 6.5. Annotation of another 25 *dpf* zebrafish from OPT 3D image using TDR-3Dbase software. In this whole-mount OPT imaging of the zebrafish, 9 parts are identified. (a) The parts of *Head*, *Eye*, *Muscle*, *Belly* and *Fin*. (b) *Blood vessel*, *Swim bladder*, *Intestine* and *Notochord & Spinal cord* are annotated within the zebrafish.

2) TDR-3Dbase and MeshLab

In Figure 6.5, another example of the annotation on a 25 *dpf* zebrafish from OPT 3D image is depicted. The annotations are done with the TDR-3Dbase [132], [142], [143] software. With TDR-3Dbase, manual annotation is well incorporated through the use of an LCD-

tablet with a pen (Wacom Cintiq). Similar to the previous results, nine labels are identified including *Eye* (blue), *Head* (light blue), *Muscle* (pink), *Belly* (dark green), *Fin* (purple), *Blood vessel* (red), *Swim bladder* (green), *Intestine* (brown) and *Notochord & Spinal cord* (yellow). As we can see from the example in Figure 6.5, TDR-3Dbase provides an informative and smooth visualization from a triangulation employing a surface rendering technique. Further refinement can be accomplished in other software. The annotation result of TDR-3Dbase is then transferred to MeshLab [145]. Now, the whole-mount zebrafish can be visualized with the volume regions (*Head*, *Muscle*, *Belly* and *Fin*) being transparent. This is depicted in Figure 6.6.
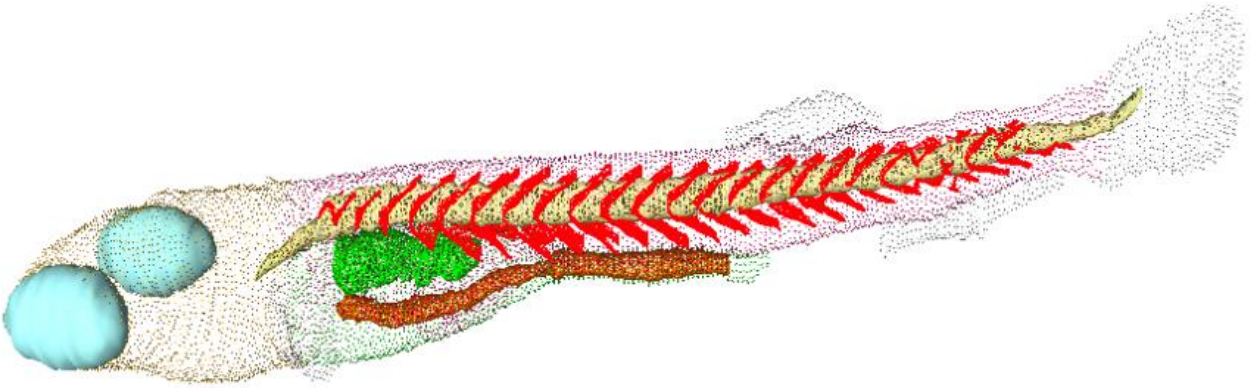

Figure 6.6. Visualization of the 25 *dpf* zebrafish using MeshLab software. The *Head*, *Muscle*, *Belly* and *Fin* are visualized as transparency in 4 different colours, whilst the *Blood vessel*, *Swim bladder*, *Intestine* and *Notochord & Spinal cord* are visualized with iso-surface technique. The mesh is obtained from TDR-3Dbase.

6.3.2 Automated 3D annotation of 5 *dpf* zebrafish

From the motivation of accelerating image analysis for zebrafish from biomedical experiments, segmentation of volume regions is explored. This has not been described in earlier literature. Inspired by the promising results achieved with 3D U-net segmentation network for binary tasks as applied in Chapter 5; i.e. on the zebrafish *Muscle* and *Eye*, we are interested in the performance for multi-label segmentation.

Different from the segmentations in Chapter 5, for a multi-label segmentation, i.e. the four volume regions we are using, the segmentation outputs four competing segmentation maps or classes excluding background. Voxels are labelled as one of the four classes that produce the highest prediction value from the segmentation network (cf. § 5.3). If this highest value is smaller than a specified threshold, the voxel will be recognized as background. The four prediction maps from the segmentation network, relevant to four volume regions accordingly, are trained from the manually labelled zebrafish in a

supervised way. The high class imbalance, e.g. *Eye* and *Muscle*, however typically results in a preferred segmentation for class with more positive samples, i.e. voxels. The learning schemas for this four-label segmentation are set similar to the approach of Chapter 5. Based on the results of Chapter 5, we use Dice loss [117] to train and validate the network on the same 35 zebrafish and test it with 3 zebrafish. The results are shown in Figure 6.7 and Table 6.1. In Figure 6.7 the qualitative performance between manual and automated segmentation on the three test zebrafish is compared. In Table 6.1 the quantitative evaluation with the five metrics similar to those used in Chapter 5 (cf. § 5.4.1) is presented. In each of the test samples, the performance of each volume region is quantified. By comparing the performance of different volume regions, it shows that the volume region *Muscle* has the highest segmentation performance with an average accuracy of 70.39% on the 3 test samples. Limited by the high class imbalance, i.e. very different numbers of voxels for the different parts, the network fails to detect the volume regions for *Eye* because it has much less voxels for the classifier.
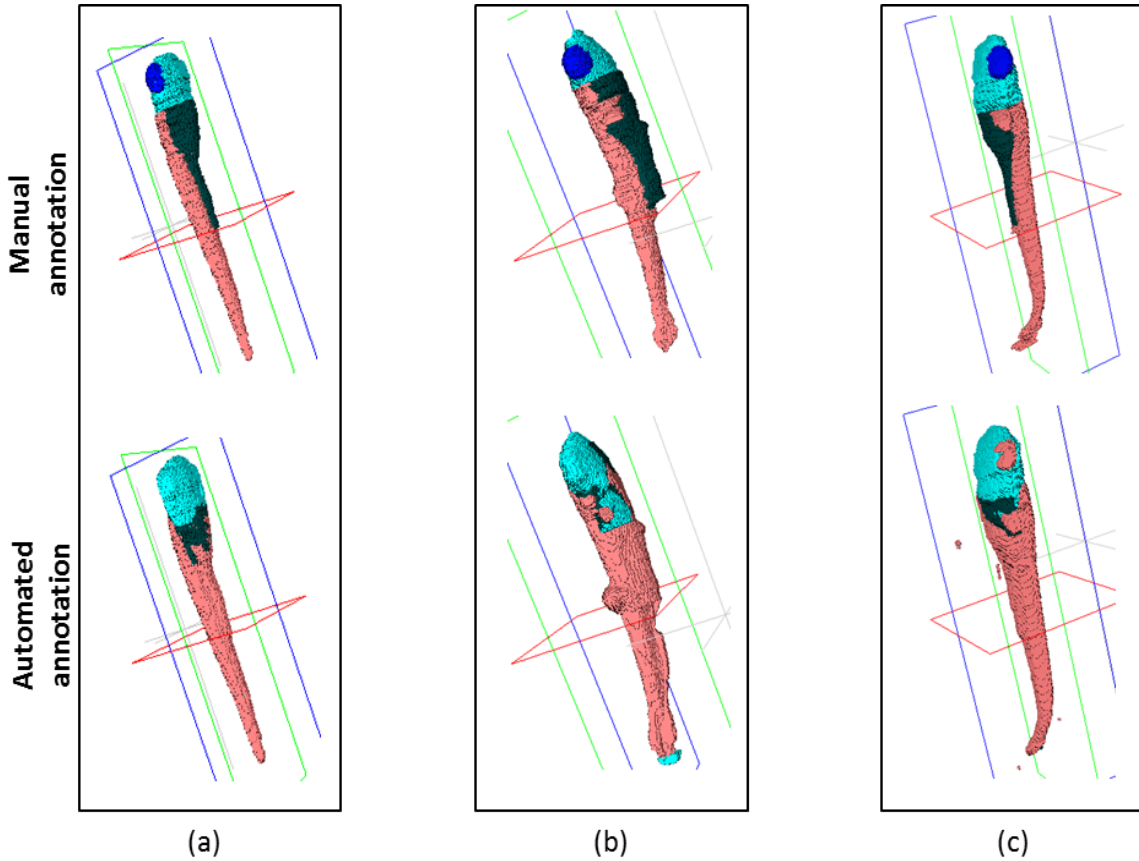

Figure 6.7. Comparisons between the performance of manual and automated segmentation on 4 parts of the 5 *dpf* zebrafish: *Eye*, *Head*, *Muscle* and *Belly*, where (a), (b) and (c) correspond to three different test samples respectively. The manually labelled models are displayed in the top row and the automated labels are in the bottom row.

Table 6.1. Quantitative evaluation of the three test samples of zebrafish. The results are obtained using the multi-label 3D U-net segmentation network. The evaluation metrics are the same as used in Chapter 5. The best performed volume region for each test sample across different metrics is printed in bold.

	Fish1(%)				Fish2(%)				Fish3(%)			
	Muscle	*Belly*	*Head*	*Eye*	*Muscle*	*Belly*	*Head*	*Eye*	*Muscle*	*Belly*	*Head*	*Eye*
DSC	**78.43**	47.22	70.82	0	**63.58**	40.15	29.64	0	**69.15**	30.12	64.41	0
Sensitivity	**91.34**	36.90	87.96	0	**85.10**	41.14	25.01	0	**96.36**	28.73	57.76	0
Specificity	99.69	**99.91**	99.66	1	99.46	99.58	**99.83**	1	99.49	99.76	**99.85**	1
F2	**85.70**	40.44	80.20	0	**74.95**	40.74	26.68	0	**83.26**	29.27	60.25	0
APR	**62.84**	24.46	52.20	0.18	**43.29**	16.51	9.39	0.17	**51.98**	9.36	42.34	0.17

6.4 Conclusions and discussion

In this chapter, we explored the last parts of our OPT imaging pipeline, the annotation and the visualization of 3D images. The outcome can be further used for phenotype characterisation. We presented examples to show to what extent the organs or regions can be annotated from a whole-mount zebrafish based on both manual and automated segmentation. With the annotation software packages, e.g. TDR-3D base [132], [142], [143], Amira [63] or Vaa3D [144], the advantage of manual annotation is that it can provide accurate segmentation including the expert-knowledge. The process is, however, quite laborious. Achieving comparable segmentation accuracies with automated annotation is challenging. Nevertheless, it can save a huge amount of labour and time. For instance, for a 3D OPT bright-field image of one single zebrafish, manual annotation normally takes hours to days depending on the level of detail. The automated annotation takes several seconds and sufficiently reasonable results are achieved. In practice, the combination of automated and manual method is recommended for an organ or volume region annotation.

With the best parameters and configurations achieved from the segmentation method described in Chapter 5, the performance for automated multi-label annotation task is not yet satisfactory. In future work further improvement need be accomplished by improving segmentation method and using larger set of images.

Based on the results, we analyse and discuss the reasons from the perspective of the data, algorithms and resources, and give further insights into performance improvement for each individual aspect. Furthermore, possible directions for further improvement are given.

1) **Data limitation**: We categorize the data limitation into three types: data characteristics, data quality and data size. Data characteristics represent the inherent structure of zebrafish as represented in a computer and it is further determined by using a specific 3D imaging technique. The data characteristic is, in proactive, determined by individual samples and imaging techniques. It defines an upper limit of the performance of segmentation of a given algorithm. Because of

the transparency of zebrafish, 3D segmentation of boundary between some parts, e.g. *Head* and *Muscle*, *Muscle* and *Belly*, in itself is challenging. The image quality related to noise in the background is segmented as foreground, with an example shown in Figure 6.7. (c). Noise is often introduced during sample preparation. Any remains, dust or bubbles during the sample preparation could result in artefacts in the 3D image. Because of the high intensity similarity between noise and some parts of zebrafish in this example, 3D U-net segmentation network fails to distinguish them when feeding the network with volume patches. In order to decrease the segmentation error resulting from noise, a cautious sample preparation process is required. With respect to data size, the performance is achieved with 35 training and validation samples. In our view this is still insufficient for training a good 3D segmentation network. To improve the segmentation performance, more zebrafish samples will be added in the next steps.

2) **Algorithm limitation**: The huge difference of performance between different parts/classes is raised by the class imbalance. The segmentation can be treated as a multi-label classifier in 3D U-net, with each voxel representing a classification sample. The segmentation task is interpreted as classifying all the voxels of a 3D image into 4 classes with a probability assigned to each class. The network fails to segment or detect the *Eye*, but it performs reasonably for *Muscle* segmentation or detection. This is probably because in all the training voxels for classification, the number of voxels as *Muscle* is much larger than that as *Eye*. This gives the *Muscle* class an unfair advantage over *Eye*. Further research and exploration that aim to solve this problem include data resampling and loss rebalancing. In data resampling, voxels of lower frequency class can be repeatedly sampled until all the classes reach to an approximate balance. Another possible solution for class imbalance would be assigning each voxel with a class weight (i.e. reciprocal of class frequency) and integrating it into prediction when implementing loss function. For both possible solutions the improvement performance need to be further verified because of the high imbalance between some classes. In 3D and multi-label classification, this imbalance research problem has become a hot and challenging topic in the recent years in medical imaging field for MRI/CT images.

3) **Resource limitation**: Constrained by the limitation of the GPU memory, the training and validation batches are fed into the network. In this way the structural and spatial information among patches are not taken into account for training. This means the smaller the patch size is, the less structures will be trained and learnt, resulting in lower performance of segmentation. In our segmentation task of four labels, the patch size is set as 64x64x64, while the image size is 128x128x340 with GPU memory size of 12GB. An increase of the GPU memory can be another improvement to the segmentation accuracy. This generally means a change of the GPU setup and it comes with a cost that need be assessed. However, given the number of different images this might be a good investment.

All considered, the research described in this chapter gives insights in future development of automation of the annotation process. In some cases, for very specific structures, a manual annotation would still be the most efficient manner of obtaining an accurate result. From the visualization examples it can be assessed that each of the software packages has its own advantages. But with a dedicated annotation software package like TDR-3Dbase [132], [142], [143], good results can be accomplished while refinements in the visualization can be accomplished with other software packages.

We have also given our considerations the respect to limitations that are imposed on the data. With time these might change, however, when method improvement is considered it is good to be aware of these limitations in an assessment for further developments.

6.5 Acknowledgement

Chapter 6